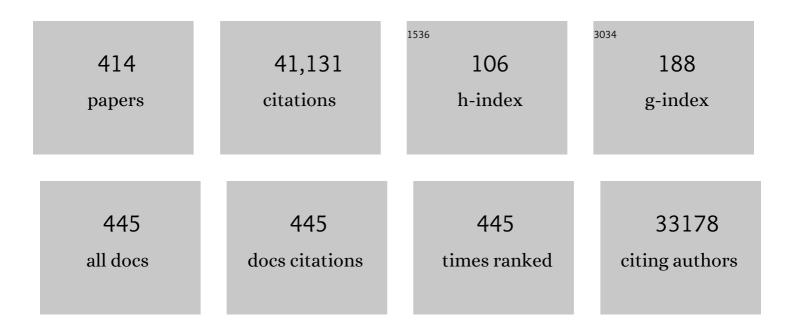
Jinlong Gong

List of Publications by Year in descending order

Source: https://exaly.com/author-pdf/1083128/publications.pdf Version: 2024-02-01



LINLONG CONC

#	Article	IF	CITATIONS
1	Recent advances in catalytic hydrogenation of carbon dioxide. Chemical Society Reviews, 2011, 40, 3703.	38.1	2,713
2	CO ₂ photo-reduction: insights into CO ₂ activation and reaction on surfaces of photocatalysts. Energy and Environmental Science, 2016, 9, 2177-2196.	30.8	1,488
3	Recent progress made in the mechanism comprehension and design of electrocatalysts for alkaline water splitting. Energy and Environmental Science, 2019, 12, 2620-2645.	30.8	1,052
4	Electrochemical sensing in paper-based microfluidic devices. Lab on A Chip, 2010, 10, 477-483.	6.0	837
5	Ethylene glycol: properties, synthesis, and applications. Chemical Society Reviews, 2012, 41, 4218.	38.1	819
6	Nanostructured Materials for Heterogeneous Electrocatalytic CO ₂ Reduction and their Related Reaction Mechanisms. Angewandte Chemie - International Edition, 2017, 56, 11326-11353.	13.8	811
7	Enhanced Surface Reaction Kinetics and Charge Separation of p–n Heterojunction Co ₃ O ₄ /BiVO ₄ Photoanodes. Journal of the American Chemical Society, 2015, 137, 8356-8359.	13.7	767
8	Sub-10 nm rutile titanium dioxide nanoparticles for efficient visible-light-driven photocatalytic hydrogen production. Nature Communications, 2015, 6, 5881.	12.8	653
9	Synthesis of Ethanol via Syngas on Cu/SiO ₂ Catalysts with Balanced Cu ⁰ –Cu ⁺ Sites. Journal of the American Chemical Society, 2012, 134, 13922-13925.	13.7	614
10	Paperâ€Based ELISA. Angewandte Chemie - International Edition, 2010, 49, 4771-4774.	13.8	610
11	Advances in solar energy conversion. Chemical Society Reviews, 2019, 48, 1862-1864.	38.1	492
12	Core–shell structured catalysts for thermocatalytic, photocatalytic, and electrocatalytic conversion of CO ₂ . Chemical Society Reviews, 2020, 49, 2937-3004.	38.1	479
13	Breaking the scaling relationship via thermally stable Pt/Cu single atom alloys for catalytic dehydrogenation. Nature Communications, 2018, 9, 4454.	12.8	451
14	Methanation of carbon dioxide: an overview. Frontiers of Chemical Science and Engineering, 2011, 5, 2-10.	4.4	443
15	Tungsten Oxide Single Crystal Nanosheets for Enhanced Multichannel Solar Light Harvesting. Advanced Materials, 2015, 27, 1580-1586.	21.0	436
16	Tantalum-based semiconductors for solar water splitting. Chemical Society Reviews, 2014, 43, 4395-4422.	38.1	421
17	Strategies for improving the performance and stability of Ni-based catalysts for reforming reactions. Chemical Society Reviews, 2014, 43, 7245-7256.	38.1	419
18	Mechanistic Understanding of the Plasmonic Enhancement for Solar Water Splitting. Advanced Materials, 2015, 27, 5328-5342.	21.0	373

#	Article	IF	CITATIONS
19	Dry reforming of methane over Ni/La2O3 nanorod catalysts with stabilized Ni nanoparticles. Applied Catalysis B: Environmental, 2017, 202, 683-694.	20.2	369
20	Promoted Fixation of Molecular Nitrogen with Surface Oxygen Vacancies on Plasmonâ€Enhanced TiO ₂ Photoelectrodes. Angewandte Chemie - International Edition, 2018, 57, 5278-5282.	13.8	365
21	Heterogeneous Molecular Systems for Photocatalytic CO ₂ Reduction with Water Oxidation. Angewandte Chemie - International Edition, 2016, 55, 14924-14950.	13.8	360
22	Propane dehydrogenation: catalyst development, new chemistry, and emerging technologies. Chemical Society Reviews, 2021, 50, 3315-3354.	38.1	354
23	Metal oxide redox chemistry for chemical looping processes. Nature Reviews Chemistry, 2018, 2, 349-364.	30.2	352
24	Theory-guided design of catalytic materials using scaling relationships and reactivity descriptors. Nature Reviews Materials, 2019, 4, 792-804.	48.7	338
25	Recent advances in capture of carbon dioxide using alkali-metal-based oxides. Energy and Environmental Science, 2011, 4, 3805.	30.8	318
26	Ceria-promoted Ni/SBA-15 catalysts for ethanol steam reforming with enhanced activity and resistance to deactivation. Applied Catalysis B: Environmental, 2015, 176-177, 532-541.	20.2	270
27	Grain-Boundary-Rich Copper for Efficient Solar-Driven Electrochemical CO ₂ Reduction to Ethylene and Ethanol. Journal of the American Chemical Society, 2020, 142, 6878-6883.	13.7	270
28	Threeâ€Phase Photocatalysis for the Enhanced Selectivity and Activity of CO ₂ Reduction on a Hydrophobic Surface. Angewandte Chemie - International Edition, 2019, 58, 14549-14555.	13.8	269
29	Effective Charge Carrier Utilization in Photocatalytic Conversions. Accounts of Chemical Research, 2016, 49, 911-921.	15.6	266
30	Controllable synthesis of nanotube-type graphitic C3N4 and their visible-light photocatalytic and fluorescent properties. Journal of Materials Chemistry A, 2014, 2, 2885.	10.3	265
31	Catalytic Reforming of Oxygenates: State of the Art and Future Prospects. Chemical Reviews, 2016, 116, 11529-11653.	47.7	258
32	A copper-phyllosilicate core-sheath nanoreactor for carbon–oxygen hydrogenolysis reactions. Nature Communications, 2013, 4, 2339.	12.8	254
33	Rational design of yolk–shell nanostructures for photocatalysis. Chemical Society Reviews, 2019, 48, 1874-1907.	38.1	254
34	Surface, Bulk, and Interface: Rational Design of Hematite Architecture toward Efficient Photoâ€Electrochemical Water Splitting. Advanced Materials, 2018, 30, e1707502.	21.0	248
35	Dendritic Au/TiO2 nanorod arrays for visible-light driven photoelectrochemical water splitting. Nanoscale, 2013, 5, 9001.	5.6	243
36	Propane Dehydrogenation over Pt/TiO ₂ –Al ₂ O ₃ Catalysts. ACS Catalysis, 2015, 5, 438-447.	11.2	243

#	Article	IF	CITATIONS
37	Morphology control of ceria nanocrystals for catalytic conversion of CO2 with methanol. Nanoscale, 2013, 5, 5582.	5.6	237
38	Synergism of Geometric Construction and Electronic Regulation: 3D Seâ€(NiCo)S <i>_x</i> /(OH) <i>_x</i> Nanosheets for Highly Efficient Overall Water Splitting. Advanced Materials, 2018, 30, e1705538.	21.0	236
39	Gradient doping of phosphorus in Fe ₂ O ₃ nanoarray photoanodes for enhanced charge separation. Chemical Science, 2017, 8, 91-100.	7.4	231
40	Theoretical insights into single-atom catalysts. Chemical Society Reviews, 2020, 49, 8156-8178.	38.1	231
41	Structure and Surface Chemistry of Gold-Based Model Catalysts. Chemical Reviews, 2012, 112, 2987-3054.	47.7	229
42	Shape-controlled synthesis of Au–Pd bimetallic nanocrystals for catalytic applications. Chemical Society Reviews, 2016, 45, 3916-3934.	38.1	228
43	Crucial Role of Surface Hydroxyls on the Activity and Stability in Electrochemical CO ₂ Reduction. Journal of the American Chemical Society, 2019, 141, 2911-2915.	13.7	217
44	Selective Deposition of Ag ₃ PO ₄ on Monoclinic BiVO ₄ (040) for Highly Efficient Photocatalysis. Small, 2013, 9, 3951-3956.	10.0	215
45	Efficient hydrogen production from ethanol steam reforming over La-modified ordered mesoporous Ni-based catalysts. Applied Catalysis B: Environmental, 2016, 181, 321-331.	20.2	213
46	Monoclinic Porous BiVO ₄ Networks Decorated by Discrete g ₃ N ₄ Nanoâ€kslands with Tunable Coverage for Highly Efficient Photocatalysis. Small, 2014, 10, 2783-2790.	10.0	209
47	Surface Science Investigations of Oxidative Chemistry on Gold. Accounts of Chemical Research, 2009, 42, 1063-1073.	15.6	206
48	Controllable fabrication of nanostructured materials for photoelectrochemical water splitting via atomic layer deposition. Chemical Society Reviews, 2014, 43, 7469-7484.	38.1	206
49	Single-Atom Mn–N ₄ Site-Catalyzed Peroxone Reaction for the Efficient Production of Hydroxyl Radicals in an Acidic Solution. Journal of the American Chemical Society, 2019, 141, 12005-12010.	13.7	203
50	The Development of Cocatalysts for Photoelectrochemical CO ₂ Reduction. Advanced Materials, 2019, 31, e1804710.	21.0	202
51	Chemoselective synthesis of ethanol via hydrogenation of dimethyl oxalate on Cu/SiO 2 : Enhanced stability with boron dopant. Journal of Catalysis, 2013, 297, 142-150.	6.2	200
52	Propane dehydrogenation over Pt–Cu bimetallic catalysts: the nature of coke deposition and the role of copper. Nanoscale, 2014, 6, 10000-10008.	5.6	191
53	Synergistic Cocatalytic Effect of Carbon Nanodots and Co ₃ O ₄ Nanoclusters for the Photoelectrochemical Water Oxidation on Hematite. Angewandte Chemie - International Edition, 2016, 55, 5851-5855.	13.8	187
54	Nano-designed semiconductors for electro- and photoelectro-catalytic conversion of carbon dioxide. Chemical Society Reviews, 2018, 47, 5423-5443.	38.1	181

#	Article	IF	CITATIONS
55	Nature of the Active Sites of VO _{<i>x</i>} /Al ₂ O ₃ Catalysts for Propane Dehydrogenation. ACS Catalysis, 2016, 6, 5207-5214.	11.2	179
56	FeO ₆ Octahedral Distortion Activates Lattice Oxygen in Perovskite Ferrite for Methane Partial Oxidation Coupled with CO ₂ Splitting. Journal of the American Chemical Society, 2020, 142, 11540-11549.	13.7	177
57	Insights into the effects of surface/bulk defects on photocatalytic hydrogen evolution over TiO2 with exposed {001} facets. Applied Catalysis B: Environmental, 2018, 220, 126-136.	20.2	176
58	Tuning Cu/Cu ₂ O Interfaces for the Reduction of Carbon Dioxide to Methanol in Aqueous Solutions. Angewandte Chemie - International Edition, 2018, 57, 15415-15419.	13.8	175
59	Water-Enhanced Low-Temperature CO Oxidation and Isotope Effects on Atomic Oxygen-Covered Au(111). Journal of the American Chemical Society, 2008, 130, 6801-6812.	13.7	171
60	Coupling of Cu(100) and (110) Facets Promotes Carbon Dioxide Conversion to Hydrocarbons and Alcohols. Angewandte Chemie - International Edition, 2021, 60, 4879-4885.	13.8	171
61	Structural motifs of water on metal oxide surfaces. Chemical Society Reviews, 2017, 46, 1785-1806.	38.1	170
62	The nature of active sites for carbon dioxide electroreduction over oxide-derived copper catalysts. Nature Communications, 2021, 12, 395.	12.8	170
63	Enriched Surface Oxygen Vacancies of Photoanodes by Photoetching with Enhanced Charge Separation. Angewandte Chemie - International Edition, 2020, 59, 2044-2048.	13.8	169
64	Sorption enhanced steam reforming of ethanol on Ni–CaO–Al2O3 multifunctional catalysts derived from hydrotalcite-like compounds. Energy and Environmental Science, 2012, 5, 8942.	30.8	168
65	Synergetic Enhancement of Light Harvesting and Charge Separation over Surface-Disorder-Engineered TiO2 Photonic Crystals. CheM, 2017, 2, 877-892.	11.7	168
66	Hydrogen Production via Steam Reforming of Ethanol on Phyllosilicate-Derived Ni/SiO ₂ : Enhanced Metal–Support Interaction and Catalytic Stability. ACS Sustainable Chemistry and Engineering, 2013, 1, 161-173.	6.7	167
67	Controllable Cu ⁰ u ⁺ Sites for Electrocatalytic Reduction of Carbon Dioxide. Angewandte Chemie - International Edition, 2021, 60, 15344-15347.	13.8	167
68	Molecular understandings on the activation of light hydrocarbons over heterogeneous catalysts. Chemical Science, 2015, 6, 4403-4425.	7.4	166
69	Hydrogen Production via Glycerol Steam Reforming over Ni/Al ₂ O ₃ : Influence of Nickel Precursors. ACS Sustainable Chemistry and Engineering, 2013, 1, 1052-1062.	6.7	164
70	Enhanced CO ₂ Electroreduction on Neighboring Zn/Co Monomers by Electronic Effect. Angewandte Chemie - International Edition, 2020, 59, 12664-12668.	13.8	164
71	Monoclinic WO3 nanomultilayers with preferentially exposed (002) facets for photoelectrochemical water splitting. Nano Energy, 2015, 11, 189-195.	16.0	162
72	Stable Aqueous Photoelectrochemical CO ₂ Reduction by a Cu ₂ O Dark Cathode with Improved Selectivity for Carbonaceous Products. Angewandte Chemie - International Edition, 2016, 55, 8840-8845.	13.8	161

#	Article	IF	CITATIONS
73	Single-crystal silicon-based electrodes for unbiased solar water splitting: current status and prospects. Chemical Society Reviews, 2019, 48, 2158-2181.	38.1	161
74	Reduced Graphene Oxide (rGO)/BiVO ₄ Composites with Maximized Interfacial Coupling for Visible Lght Photocatalysis. ACS Sustainable Chemistry and Engineering, 2014, 2, 2253-2258.	6.7	159
75	An Alternative Synthetic Approach for Efficient Catalytic Conversion of Syngas to Ethanol. Accounts of Chemical Research, 2014, 47, 1483-1492.	15.6	159
76	Platinum-Modified ZnO/Al ₂ O ₃ for Propane Dehydrogenation: Minimized Platinum Usage and Improved Catalytic Stability. ACS Catalysis, 2016, 6, 2158-2162.	11.2	159
77	<i>Operando</i> characterization techniques for electrocatalysis. Energy and Environmental Science, 2020, 13, 3748-3779.	30.8	159
78	Strong Electronic Oxide–Support Interaction over In ₂ O ₃ /ZrO ₂ for Highly Selective CO ₂ Hydrogenation to Methanol. Journal of the American Chemical Society, 2020, 142, 19523-19531.	13.7	156
79	Recent Advances on the Design of Group VIII Base-Metal Catalysts with Encapsulated Structures. ACS Catalysis, 2015, 5, 4959-4977.	11.2	150
80	Thin Heterojunctions and Spatially Separated Cocatalysts To Simultaneously Reduce Bulk and Surface Recombination in Photocatalysts. Angewandte Chemie - International Edition, 2016, 55, 13734-13738.	13.8	149
81	Hydroxylâ€Mediated Nonâ€oxidative Propane Dehydrogenation over VO _{<i>x</i>} /γâ€Al ₂ O ₃ Catalysts with Improved Stability. Angewandte Chemie - International Edition, 2018, 57, 6791-6795.	13.8	149
82	Dendritic Hematite Nanoarray Photoanode Modified with a Conformal Titanium Dioxide Interlayer for Effective Charge Collection. Angewandte Chemie - International Edition, 2017, 56, 12878-12882.	13.8	143
83	Ultrathin Pd–Au Shells with Controllable Alloying Degree on Pd Nanocubes toward Carbon Dioxide Reduction. Journal of the American Chemical Society, 2019, 141, 4791-4794.	13.7	142
84	Selective Oxidation of Ethanol to Acetaldehyde on Gold. Journal of the American Chemical Society, 2008, 130, 16458-16459.	13.7	141
85	Glycerol steam reforming over perovskite-derived nickel-based catalysts. Applied Catalysis B: Environmental, 2014, 144, 277-285.	20.2	141
86	Hydroxyl-mediated ethanol selectivity of CO ₂ hydrogenation. Chemical Science, 2019, 10, 3161-3167.	7.4	138
87	Enhanced Lattice Oxygen Reactivity over Ni-Modified WO ₃ -Based Redox Catalysts for Chemical Looping Partial Oxidation of Methane. ACS Catalysis, 2017, 7, 3548-3559.	11.2	136
88	Modulating Lattice Oxygen in Dual-Functional Mo–V–O Mixed Oxides for Chemical Looping Oxidative Dehydrogenation. Journal of the American Chemical Society, 2019, 141, 18653-18657.	13.7	133
89	Surviving Highâ€Temperature Calcination: ZrO ₂ â€Induced Hematite Nanotubes for Photoelectrochemical Water Oxidation. Angewandte Chemie - International Edition, 2017, 56, 4150-4155.	13.8	132
90	Au nanoparticle sensitized ZnO nanopencil arrays for photoelectrochemical water splitting. Nanoscale, 2015, 7, 77-81.	5.6	131

#	Article	IF	CITATIONS
91	Spatial separation of oxidation and reduction co-catalysts for efficient charge separation: Pt@TiO ₂ @MnO _x hollow spheres for photocatalytic reactions. Chemical Science, 2016, 7, 890-895.	7.4	130
92	Low oordinated Edge Sites on Ultrathin Palladium Nanosheets Boost Carbon Dioxide Electroreduction Performance. Angewandte Chemie - International Edition, 2018, 57, 11544-11548.	13.8	127
93	Adjusting the Reduction Potential of Electrons by Quantum Confinement for Selective Photoreduction of CO ₂ to Methanol. Angewandte Chemie - International Edition, 2019, 58, 3804-3808.	13.8	126
94	Hydrogenation of dimethyl oxalate to ethylene glycol on a Cu/SiO ₂ /cordierite monolithic catalyst: Enhanced internal mass transfer and stability. AICHE Journal, 2012, 58, 2798-2809.	3.6	125
95	Enhanced Charge Separation through ALDâ€Modified Fe ₂ O ₃ /Fe ₂ TiO ₅ Nanorod Heterojunction for Photoelectrochemical Water Oxidation. Small, 2016, 12, 3415-3422.	10.0	124
96	Phosgene-free approaches to catalytic synthesis of diphenyl carbonate and its intermediates. Applied Catalysis A: General, 2007, 316, 1-21.	4.3	123
97	Singleâ€Crystal Semiconductors with Narrow Band Gaps for Solar Water Splitting. Angewandte Chemie - International Edition, 2015, 54, 10718-10732.	13.8	123
98	Activation and Spillover of Hydrogen on Subâ€1 nm Palladium Nanoclusters Confined within Sodalite Zeolite for the Semiâ€Hydrogenation of Alkynes. Angewandte Chemie - International Edition, 2019, 58, 7668-7672.	13.8	123
99	Homogeneous Cu2O p-n junction photocathodes for solar water splitting. Applied Catalysis B: Environmental, 2018, 226, 31-37.	20.2	121
100	Propane Dehydrogenation on Single-Site [PtZn4] Intermetallic Catalysts. CheM, 2021, 7, 387-405.	11.7	116
101	Edge Sites with Unsaturated Coordination on Core–Shell Mn ₃ O ₄ @Mn <i>_x</i> Co _{3â^²} <i>_x4/i>O_{4<!--<br-->Nanostructures for Electrocatalytic Water Oxidation. Advanced Materials, 2017, 29, 1701820.}</i>	subt>0	115
102	Surface Chemistry of Methanol on Clean and Atomic Oxygen Pre-Covered Au(111). Journal of Physical Chemistry C, 2008, 112, 5501-5509.	3.1	114
103	Spatial control of cocatalysts and elimination of interfacial defects towards efficient and robust CIGS photocathodes for solar water splitting. Energy and Environmental Science, 2018, 11, 2025-2034.	30.8	114
104	Dimensional construction and morphological tuning of heterogeneous MoS ₂ /NiS electrocatalysts for efficient overall water splitting. Journal of Materials Chemistry A, 2018, 6, 9833-9838.	10.3	114
105	Selectivity Modulation of Encapsulated Palladium Nanoparticles by Zeolite Microenvironment for Biomass Catalytic Upgrading. ACS Catalysis, 2018, 8, 8578-8589.	11.2	114
106	Photoelectrochemical CO ₂ reduction to adjustable syngas on grain-boundary-mediated a-Si/TiO ₂ /Au photocathodes with low onset potentials. Energy and Environmental Science, 2019, 12, 923-928.	30.8	114
107	A Ni@ZrO ₂ nanocomposite for ethanol steam reforming: enhanced stability via strong metal–oxide interaction. Chemical Communications, 2013, 49, 4226-4228.	4.1	112
108	Branched TiO2 nanoarrays sensitized with CdS quantum dots for highly efficient photoelectrochemical water splitting. Physical Chemistry Chemical Physics, 2013, 15, 12026.	2.8	109

#	Article	IF	CITATIONS
109	Gold Nanorod@TiO ₂ Yolkâ€Shell Nanostructures for Visibleâ€Lightâ€Driven Photocatalytic Oxidation of Benzyl Alcohol. Small, 2015, 11, 1892-1899.	10.0	109
110	Insights into interface engineering in steam reforming reactions for hydrogen production. Energy and Environmental Science, 2019, 12, 3473-3495.	30.8	109
111	Efficient CO2 electroreduction on facet-selective copper films with high conversion rate. Nature Communications, 2021, 12, 5745.	12.8	108
112	Water Activated by Atomic Oxygen on Au(111) to Oxidize CO at Low Temperatures. Journal of the American Chemical Society, 2006, 128, 6282-6283.	13.7	106
113	Identification of Pt-based catalysts for propane dehydrogenation <i>via</i> a probability analysis. Chemical Science, 2018, 9, 3925-3931.	7.4	106
114	Gold nanorods-based hybrids with tailored structures for photoredox catalysis: fundamental science, materials design and applications. Nano Today, 2019, 27, 48-72.	11.9	104
115	Tunable Magnetism in Carbon″on″mplanted Highly Oriented Pyrolytic Graphite. Advanced Materials, 2008, 20, 4679-4683.	21.0	103
116	Bubble-supported engineering of hierarchical CuCo ₂ S ₄ hollow spheres for enhanced electrochemical performance. Journal of Materials Chemistry A, 2018, 6, 5265-5270.	10.3	103
117	Nanostrukturierte Materialien für die elektrokatalytische CO ₂ â€Reduktion und ihre Reaktionsmechanismen. Angewandte Chemie, 2017, 129, 11482-11511.	2.0	102
118	Sintering-resistant Ni-based reforming catalysts obtained via the nanoconfinement effect. Chemical Communications, 2013, 49, 9383.	4.1	101
119	WO ₃ photoanodes with controllable bulk and surface oxygen vacancies for photoelectrochemical water oxidation. Journal of Materials Chemistry A, 2018, 6, 3350-3354.	10.3	100
120	Mesoporous anatase TiO2 nanocups with plasmonic metal decoration for highly active visible-light photocatalysis. Chemical Communications, 2013, 49, 5817.	4.1	99
121	Coupling of Cu(100) and (110) Facets Promotes Carbon Dioxide Conversion to Hydrocarbons and Alcohols. Angewandte Chemie, 2021, 133, 4929-4935.	2.0	98
122	Dry reforming of methane over La2O2CO3-modified Ni/Al2O3 catalysts with moderate metal support interaction. Applied Catalysis B: Environmental, 2020, 264, 118448.	20.2	95
123	Understanding electronic and optical properties of anatase TiO2 photocatalysts co-doped with nitrogen and transition metals. Physical Chemistry Chemical Physics, 2013, 15, 9549.	2.8	93
124	Tunable syngas production from photocatalytic CO ₂ reduction with mitigated charge recombination driven by spatially separated cocatalysts. Chemical Science, 2018, 9, 5334-5340.	7.4	89
125	Subsurface catalysis-mediated selectivity of dehydrogenation reaction. Science Advances, 2018, 4, eaar5418.	10.3	89
126	Ordered mesoporous Ni/La2O3 catalysts with interfacial synergism towards CO2 activation in dry reforming of methane. Applied Catalysis B: Environmental, 2019, 259, 118092.	20.2	89

#	Article	IF	CITATIONS
127	PEGylated liposome coated QDs/mesoporous silica core-shell nanoparticles for molecular imaging. Chemical Communications, 2011, 47, 3442.	4.1	88
128	Formation of Enriched Vacancies for Enhanced CO ₂ Electrocatalytic Reduction over AuCu Alloys. ACS Energy Letters, 2018, 3, 2144-2149.	17.4	88
129	Catalytic hydrothermal liquefaction for bio-oil production over CNTs supported metal catalysts. Chemical Engineering Science, 2017, 161, 299-307.	3.8	87
130	Current Mechanistic Understanding of Surface Reactions over Water-Splitting Photocatalysts. CheM, 2018, 4, 223-245.	11.7	87
131	Broadband Light Harvesting and Unidirectional Electron Flow for Efficient Electron Accumulation for Hydrogen Generation. Angewandte Chemie - International Edition, 2019, 58, 10003-10007.	13.8	86
132	Hydrogenation of dimethyl oxalate to ethylene glycol over mesoporous <scp><scp>Cu</scp></scp> â€ <scp>MCM</scp> â€41 catalysts. AICHE Journal, 2013, 59, 2530-2539.	3.6	85
133	Morphological and Compositional Design of Pd–Cu Bimetallic Nanocatalysts with Controllable Product Selectivity toward CO ₂ Electroreduction. Small, 2018, 14, 1703314.	10.0	84
134	The Interplay between Structure and Product Selectivity of CO ₂ Hydrogenation. Angewandte Chemie - International Edition, 2019, 58, 11242-11247.	13.8	84
135	Two-dimensional gersiloxenes with tunable bandgap for photocatalytic H2 evolution and CO2 photoreduction to CO. Nature Communications, 2020, 11, 1443.	12.8	84
136	Selective Catalytic Oxidation of Ammonia to Nitrogen on Atomic Oxygen Precovered Au(111). Journal of the American Chemical Society, 2006, 128, 9012-9013.	13.7	83
137	The Functionality of Surface Hydroxy Groups on the Selectivity and Activity of Carbon Dioxide Reduction over Cuprous Oxide in Aqueous Solutions. Angewandte Chemie - International Edition, 2018, 57, 7724-7728.	13.8	82
138	Steam reforming of ethanol over Ni/ZrO2 catalysts: Effect of support on product distribution. International Journal of Hydrogen Energy, 2012, 37, 2940-2949.	7.1	81
139	Facile synthesis of ZnO nanopencil arrays for photoelectrochemical water splitting. Nano Energy, 2014, 7, 143-150.	16.0	79
140	Effects of Ga doping on Pt/CeO ₂ â€Al ₂ O ₃ catalysts for propane dehydrogenation. AICHE Journal, 2016, 62, 4365-4376.	3.6	79
141	Structure–Performance Relationships for Propane Dehydrogenation over Aluminum Supported Vanadium Oxide. ACS Catalysis, 2019, 9, 5816-5827.	11.2	76
142	Micro- and Nanopatterning of Inorganic and Polymeric Substrates by Indentation Lithography. Nano Letters, 2010, 10, 2702-2708.	9.1	72
143	A General Approach to Synthesize Asymmetric Hybrid Nanoparticles by Interfacial Reactions. Journal of the American Chemical Society, 2012, 134, 3639-3642.	13.7	72
144	Enhanced oxygen mobility and reactivity for ethanol steam reforming. AICHE Journal, 2012, 58, 516-525.	3.6	70

#	Article	IF	CITATIONS
145	Bifacial passivation of <i>n</i> -silicon metal–insulator–semiconductor photoelectrodes for efficient oxygen and hydrogen evolution reactions. Energy and Environmental Science, 2020, 13, 221-228.	30.8	70
146	Selective Oxidation of Propanol on Au(111): Mechanistic Insights into Aerobic Oxidation of Alcohols. ChemPhysChem, 2008, 9, 2461-2466.	2.1	67
147	CeO ₂ -modified Au@SBA-15 nanocatalysts for liquid-phase selective oxidation of benzyl alcohol. Nanoscale, 2015, 7, 7593-7602.	5.6	67
148	Hydrogenated Cagelike Titania Hollow Spherical Photocatalysts for Hydrogen Evolution under Simulated Solar Light Irradiation. ACS Applied Materials & Interfaces, 2016, 8, 23006-23014.	8.0	67
149	Unraveling the rate-limiting step of two-electron transfer electrochemical reduction of carbon dioxide. Nature Communications, 2022, 13, 803.	12.8	67
150	Fabrication of porous nanoflake BiMO _x (M = W, V, and Mo) photoanodes via hydrothermal anion exchange. Chemical Science, 2016, 7, 6381-6386.	7.4	65
151	Investigation of carbon fiber reinforced polymer (CFRP) sheet with subsurface defects inspection using thermal-wave radar imaging (TWRI) based on the multi-transform technique. NDT and E International, 2014, 62, 130-136.	3.7	64
152	Facilitating the reduction of V–O bonds on VO _x /ZrO ₂ catalysts for non-oxidative propane dehydrogenation. Chemical Science, 2020, 11, 3845-3851.	7.4	63
153	Etching effects of ethanol on multi-walled carbon nanotubes. Carbon, 2006, 44, 1218-1224.	10.3	61
154	Highly-oriented Fe ₂ O ₃ /ZnFe ₂ O ₄ nanocolumnar heterojunction with improved charge separation for photoelectrochemical water oxidation. Chemical Communications, 2016, 52, 9013-9015.	4.1	61
155	Nanostructured NiFe (oxy)hydroxide with easily oxidized Ni towards efficient oxygen evolution reactions. Journal of Materials Chemistry A, 2018, 6, 16810-16817.	10.3	61
156	Sorption enhanced steam reforming of methanol for high-purity hydrogen production over Cu-MgO/Al2O3 bifunctional catalysts. Applied Catalysis B: Environmental, 2020, 276, 119052.	20.2	61
157	Multifunctional TiO2 overlayer for p-Si/n-CdS heterojunction photocathode with improved efficiency and stability. Nano Energy, 2018, 53, 125-129.	16.0	60
158	Selective oxidation of methanol to dimethoxymethane over bifunctional VOx/TS-1 catalysts. Chemical Communications, 2011, 47, 9345.	4.1	59
159	Synthesis of stable Ni-CeO2 catalysts via ball-milling for ethanol steam reforming. Catalysis Today, 2014, 233, 53-60.	4.4	59
160	Selective oxidation of methanol to dimethoxymethane on V2O5–MoO3/γ-Al2O3 catalysts. Applied Catalysis B: Environmental, 2014, 160-161, 161-172.	20.2	59
161	Porous single-crystalline AuPt@Pt bimetallic nanocrystals with high mass electrocatalytic activities. Chemical Science, 2016, 7, 3500-3505.	7.4	59
162	Symmetry-Breaking Synthesis of Multicomponent Nanoparticles. Accounts of Chemical Research, 2019, 52, 1125-1133.	15.6	58

#	Article	IF	CITATIONS
163	Nanostructured Catalysts toward Efficient Propane Dehydrogenation. Accounts of Materials Research, 2020, 1, 30-40.	11.7	58
164	Near-infrared light-responsive vesicles of Au nanoflowers. Chemical Communications, 2013, 49, 576-578.	4.1	57
165	Coverageâ€Dependent Behaviors of Vanadium Oxides for Chemical Looping Oxidative Dehydrogenation. Angewandte Chemie - International Edition, 2020, 59, 22072-22079.	13.8	57
166	Chemical looping oxidative steam reforming of methanol: A new pathway for auto-thermal conversion. Applied Catalysis B: Environmental, 2020, 269, 118758.	20.2	57
167	Shale gas revolution: Catalytic conversion of C1–C3 light alkanes to value-added chemicals. CheM, 2021, 7, 1755-1801.	11.7	57
168	The nature of surface acidity and reactivity of MoO3/SiO2 and MoO3/TiO2–SiO2 for transesterification of dimethyl oxalate with phenol: A comparative investigation. Applied Catalysis B: Environmental, 2007, 77, 125-134.	20.2	56
169	Millimeter-scale contact printing of aqueous solutions using a stamp made out of paper and tape. Lab on A Chip, 2010, 10, 3201.	6.0	56
170	Achieving efficient and robust catalytic reforming on dual-sites of Cu species. Chemical Science, 2019, 10, 2578-2584.	7.4	56
171	The Interplay between Structure and Product Selectivity of CO ₂ Hydrogenation. Angewandte Chemie, 2019, 131, 11364-11369.	2.0	55
172	Reactivity and surface properties of silica supported molybdenum oxide catalysts for the transesterification of dimethyl oxalate with phenol. Catalysis Communications, 2004, 5, 101-106.	3.3	54
173	Transparent ALD-grown Ta ₂ O ₅ protective layer for highly stable ZnO photoelectrode in solar water splitting. Chemical Communications, 2015, 51, 7290-7293.	4.1	54
174	Highly loaded Ni-based catalysts for low temperature ethanol steam reforming. Nanoscale, 2016, 8, 10177-10187.	5.6	54
175	The role of Al doping in Pd/ZnO catalyst for CO2 hydrogenation to methanol. Applied Catalysis B: Environmental, 2020, 263, 118367.	20.2	54
176	Defect-promoted visible light-driven C C coupling reactions pairing with CO2 reduction. Journal of Catalysis, 2020, 390, 244-250.	6.2	54
177	Tuning Oxygen Vacancies of Oxides to Promote Electrocatalytic Reduction of Carbon Dioxide. ACS Energy Letters, 2020, 5, 552-558.	17.4	54
178	On the Role of Sn Segregation of Pt-Sn Catalysts for Propane Dehydrogenation. ACS Catalysis, 2021, 11, 4401-4410.	11.2	54
179	A Low ost NiO Hole Transfer Layer for Ohmic Back Contact to Cu ₂ O for Photoelectrochemical Water Splitting. Small, 2017, 13, 1702007.	10.0	53
180	Enhanced CO ₂ adsorption capacity and stability using CaOâ€based adsorbents treated by hydration. AICHE Journal, 2013, 59, 3586-3593.	3.6	52

#	Article	IF	CITATIONS
181	N-doped Ag/TiO ₂ hollow spheres for highly efficient photocatalysis under visible-light irradiation. RSC Advances, 2013, 3, 720-724.	3.6	52
182	On the role of Ce in CO ₂ adsorption and activation over lanthanum species. Chemical Science, 2018, 9, 3426-3437.	7.4	51
183	Alternative Strategies Toward Sustainable Ammonia Synthesis. Transactions of Tianjin University, 2020, 26, 67-91.	6.4	51
184	Asymmetric organic/metal(oxide) hybrid nanoparticles: synthesis and applications. Nanoscale, 2013, 5, 5151.	5.6	50
185	Performance evaluation of sorption enhanced chemical-looping reforming for hydrogen production from biomass with modification of catalyst and sorbent regeneration. Chemical Engineering Journal, 2016, 303, 338-347.	12.7	50
186	Enhancement of photoelectrochemical oxidation by an amorphous nickel boride catalyst on porous BiVO ₄ . Nanoscale, 2017, 9, 16133-16137.	5.6	50
187	Competition of C bond formation and Câ€H bond formation For acetylene hydrogenation on transition metals: A density functional theory study. AICHE Journal, 2019, 65, 1059-1066.	3.6	50
188	Pt–Cu Interaction Induced Construction of Single Pt Sites for Synchronous Electron Capture and Transfer in Photocatalysis. Advanced Functional Materials, 2021, 31, 2104343.	14.9	50
189	Synthesis of Platinum Nanotubes and Nanorings via Simultaneous Metal Alloying and Etching. Journal of the American Chemical Society, 2016, 138, 6332-6335.	13.7	49
190	Threeâ€Phase Photocatalysis for the Enhanced Selectivity and Activity of CO ₂ Reduction on a Hydrophobic Surface. Angewandte Chemie, 2019, 131, 14691-14697.	2.0	49
191	Stable Aqueous Photoelectrochemical CO ₂ Reduction by a Cu ₂ O Dark Cathode with Improved Selectivity for Carbonaceous Products. Angewandte Chemie, 2016, 128, 8986-8991.	2.0	48
192	Surviving Highâ€Temperature Calcination: ZrO ₂ â€Induced Hematite Nanotubes for Photoelectrochemical Water Oxidation. Angewandte Chemie, 2017, 129, 4214-4219.	2.0	48
193	Structure and catalytic consequence of Mgâ€modified VO _x /Al ₂ O ₃ catalysts for propane dehydrogenation. AICHE Journal, 2017, 63, 4911-4919.	3.6	47
194	Fabrication of bilayer Pd-Pt nanocages with sub-nanometer thin shells for enhanced hydrogen evolution reaction. Nano Research, 2019, 12, 2268-2274.	10.4	47
195	Heterogene molekulare Systeme für eine photokatalytische CO ₂ â€Reduktion mit Wasseroxidation. Angewandte Chemie, 2016, 128, 15146-15174.	2.0	46
196	Abundant Ce ³⁺ lons in Auâ€CeO <i>_x</i> Nanosheets to Enhance CO ₂ Electroreduction Performance. Small, 2019, 15, e1900289.	10.0	46
197	Hydrogen production via chemical looping steam reforming of ethanol by Ni-based oxygen carriers supported on CeO2 and La2O3 promoted Al2O3. International Journal of Hydrogen Energy, 2020, 45, 1477-1491.	7.1	46
198	Passivation of surface states by ALD-grown TiO ₂ overlayers on Ta ₃ N ₅ anodes for photoelectrochemical water oxidation. Chemical Communications, 2016, 52, 8806-8809.	4.1	45

#	Article	IF	CITATIONS
199	Fundamental insights into interfacial catalysis. Chemical Society Reviews, 2017, 46, 1770-1771.	38.1	45
200	Promoted Fixation of Molecular Nitrogen with Surface Oxygen Vacancies on Plasmonâ€Enhanced TiO ₂ Photoelectrodes. Angewandte Chemie, 2018, 130, 5376-5380.	2.0	45
201	Low temperature CO oxidation on Au(111) and the role of adsorbed water. Topics in Catalysis, 2007, 44, 57-63.	2.8	44
202	Catalysis for production of renewable energy. Chemical Society Reviews, 2014, 43, 7466-7468.	38.1	44
203	Bridging the transport pathway of charge carriers in a Ta ₃ N ₅ nanotube array photoanode for solar water splitting. Nanoscale, 2015, 7, 13153-13158.	5.6	44
204	Improved Oxygen Evolution Kinetics and Surface States Passivation of Ni-B i Co-Catalyst for a Hematite Photoanode. Engineering, 2017, 3, 285-289.	6.7	44
205	Crystal structures, acid–base properties, and reactivities of CexZr1â^'xO2 catalysts. Catalysis Today, 2009, 148, 323-328.	4.4	43
206	Synergistic Cocatalytic Effect of Carbon Nanodots and Co ₃ O ₄ Nanoclusters for the Photoelectrochemical Water Oxidation on Hematite. Angewandte Chemie, 2016, 128, 5945-5949.	2.0	42
207	A highly efficient photoelectrochemical H ₂ O ₂ production reaction with Co ₃ O ₄ as a co-catalyst. Chemical Communications, 2018, 54, 7026-7029.	4.1	42
208	Enriched Surface Oxygen Vacancies of Photoanodes by Photoetching with Enhanced Charge Separation. Angewandte Chemie, 2020, 132, 2060-2064.	2.0	41
209	Chemical looping steam reforming of methane over Ce-doped perovskites. Chemical Engineering Science, 2020, 223, 115707.	3.8	41
210	Imaging Hindered Rotations of Alkoxy Species on TiO2(110). Journal of the American Chemical Society, 2009, 131, 17926-17932.	13.7	40
211	Molecular heterogeneous catalysts derived from bipyridine-based organosilica nanotubes for C–H bond activation. Chemical Science, 2017, 8, 4489-4496.	7.4	40
212	Facet-evolution growth of Mn3O4@CoxMn3-xO4 electrocatalysts on Ni foam towards efficient oxygen evolution reaction. Journal of Catalysis, 2019, 369, 105-110.	6.2	40
213	Carbonate Formation and Decomposition on Atomic Oxygen Precovered Au(111). Journal of the American Chemical Society, 2008, 130, 11250-11251.	13.7	39
214	Synthesis of Pd nanoparticles supported on CeO2 nanotubes for CO oxidation at low temperatures. Chinese Journal of Catalysis, 2016, 37, 83-90.	14.0	39
215	Lowâ€Coordinated Edge Sites on Ultrathin Palladium Nanosheets Boost Carbon Dioxide Electroreduction Performance. Angewandte Chemie, 2018, 130, 11718-11722.	2.0	39
216	Power-to-X: Lighting the Path to a Net-Zero-Emission Future. ACS Sustainable Chemistry and Engineering, 2021, 9, 7179-7181.	6.7	39

#	Article	IF	CITATIONS
217	Steam reforming of ethanol over skeletal Niâ€based catalysts: A temperature programmed desorption and kinetic study. AICHE Journal, 2014, 60, 635-644.	3.6	38
218	Water Splitting: Synergism of Geometric Construction and Electronic Regulation: 3D Seâ€(NiCo)S <i>_x</i> /(OH) <i>_x</i> Nanosheets for Highly Efficient Overall Water Splitting (Adv. Mater. 12/2018). Advanced Materials, 2018, 30, 1870085.	21.0	38
219	Multifunctional Nickel Film Protected nâ€Type Silicon Photoanode with High Photovoltage for Efficient and Stable Oxygen Evolution Reaction. Small Methods, 2019, 3, 1900212.	8.6	38
220	On the origin of reactivity of steam reforming of ethylene glycol on supported Ni catalysts. Physical Chemistry Chemical Physics, 2012, 14, 4066.	2.8	37
221	Cu-doped zeolites for catalytic oxidative carbonylation: The role of BrÃ,nsted acids. Applied Catalysis A: General, 2012, 417-418, 236-242.	4.3	37
222	Tunable metal-oxide interaction with balanced Ni0/Ni2+ sites of Ni Mg1â^'O for ethanol steam reforming. Applied Catalysis B: Environmental, 2021, 293, 120178.	20.2	37
223	Liquidâ€phase hydrogenation of cinnamaldehyde over Cuâ€Au/SiO ₂ catalysts. AICHE Journal, 2014, 60, 3300-3311.	3.6	35
224	Active sites in CO2 hydrogenation over confined VOx-Rh catalysts. Science China Chemistry, 2019, 62, 1710-1719.	8.2	35
225	Superior reactivity of skeletal Ni-based catalysts for low-temperature steam reforming to produce CO-free hydrogen. Physical Chemistry Chemical Physics, 2012, 14, 3295.	2.8	34
226	Advancing the Use of Sustainability Metrics in <i>ACS Sustainable Chemistry & Engineering</i> . ACS Sustainable Chemistry and Engineering, 2018, 6, 1-1.	6.7	34
227	Achieving convenient CO ₂ electroreduction and photovoltage in tandem using potential-insensitive disordered Ag nanoparticles. Chemical Science, 2018, 9, 6599-6604.	7.4	34
228	Facet design promotes electroreduction of carbon dioxide to carbon monoxide on palladium nanocrystals. Chemical Engineering Science, 2019, 194, 29-35.	3.8	34
229	Characterization and catalytic activity of TiO2/SiO2 for transesterification of dimethyl oxalate with phenol. Journal of Molecular Catalysis A, 2004, 214, 273-279.	4.8	33
230	Constructing carbon nanotube junctions by Ar ion beam irradiation. Radiation Physics and Chemistry, 2010, 79, 687-691.	2.8	33
231	The Nature of Loading-Dependent Reaction Barriers over Mixed RuO ₂ /TiO ₂ Catalysts. ACS Catalysis, 2018, 8, 5526-5532.	11.2	33
232	Controllable Cu ⁰ u ⁺ Sites for Electrocatalytic Reduction of Carbon Dioxide. Angewandte Chemie, 2021, 133, 15472-15475.	2.0	33
233	Nature of the Active Sites of Copper Zinc Catalysts for Carbon Dioxide Electroreduction. Angewandte Chemie - International Edition, 2022, 61, .	13.8	33
234	Oxygen Exchange in the Selective Oxidation of 2-Butanol on Oxygen Precovered Au(111). Journal of the American Chemical Society, 2009, 131, 16189-16194.	13.7	32

#	Article	IF	CITATIONS
235	Selective oxidation of propylamine to propionitrile and propionaldehyde on oxygen-covered gold. Chemical Communications, 2009, , 761.	4.1	32
236	Model Studies with Gold: A Versatile Oxidation and Hydrogenation Catalyst. Accounts of Chemical Research, 2014, 47, 750-760.	15.6	32
237	Structural evolution of concave trimetallic nanocubes with tunable ultra-thin shells for oxygen reduction reaction. Nanoscale, 2016, 8, 16640-16649.	5.6	32
238	Collapsed polymer-directed synthesis of multicomponent coaxial-like nanostructures. Nature Communications, 2016, 7, 12147.	12.8	32
239	Tuning Cu/Cu 2 O Interfaces for the Reduction of Carbon Dioxide to Methanol in Aqueous Solutions. Angewandte Chemie, 2018, 130, 15641-15645.	2.0	32
240	Vacancy-Assisted Diffusion of Alkoxy Species on Rutile <mml:math xmlns:mml="http://www.w3.org/1998/Math/MathML" display="inline"><mml:msub><mml:mi>TiO</mml:mi><mml:mn>2</mml:mn></mml:msub><mml:mo stretchy="false">(<ml:mn>110<ml:mo) 0="" 10="" 50="" 527="" etqq0="" overlock="" rgbt="" td="" td<="" tf="" tj=""><td>7.8 (stretchy=</td><td>31 "false">)</td></ml:mo)></ml:mn></mml:mo </mml:math 	7.8 (stretchy=	31 "false">)
241	CaO-based meshed hollow spheres for CO 2 capture. Chemical Engineering Science, 2015, 135, 532-539.	3.8	31
242	Selective atomic layer deposition of RuO _x catalysts on shape-controlled Pd nanocrystals with significantly enhanced hydrogen evolution activity. Journal of Materials Chemistry A, 2018, 6, 24397-24406.	10.3	31
243	Promotional role of MgO on sorptionâ€enhanced steam reforming of ethanol over Ni/CaO catalysts. AICHE Journal, 2020, 66, e16877.	3.6	31
244	Pt-based core–shell nanocatalysts with enhanced activity and stability for CO oxidation. Chemical Communications, 2013, 49, 10647.	4.1	30
245	Dynamics of Heterogeneous Catalytic Processes at Operando Conditions. Jacs Au, 2021, 1, 2100-2120.	7.9	30
246	A Transparent, Highâ€Performance, and Stable Sb ₂ S ₃ Photoanode Enabled by Heterojunction Engineering with Conjugated Polycarbazole Frameworks for Unbiased Photoelectrochemical Overall Water Splitting Devices. Advanced Materials, 2022, 34, e2200723.	21.0	30
247	Fabrication of carbon nanowire networks by Si ion beam irradiation. Applied Physics Letters, 2006, 89, 053107.	3.3	29
248	Tuning Porosity of Ti-MCM-41: Implication for Shape Selective Catalysis. ACS Applied Materials & Interfaces, 2011, 3, 2154-2160.	8.0	29
249	Mechanistic Insights into Selective Oxidation of Ethanol on Au(111): A DFT Study. Chinese Journal of Catalysis, 2012, 33, 407-415.	14.0	29
250	Facile synthesis of functional Au nanopatches and nanocups. Chemical Communications, 2012, 48, 7344.	4.1	29
251	The Effects of Adsorbed Water on Gold Catalysis and Surface Chemistry. Topics in Catalysis, 2013, 56, 1499-1511.	2.8	29
252	Fluorescent hydroxyapatiteâ€loaded biodegradable polymer nanoparticles with folate decoration for targeted imaging. AICHE Journal, 2013, 59, 4494-4501.	3.6	29

#	Article	IF	CITATIONS
253	Selective Oxidation of Methanol to Dimethoxymethane over Mesoporous Alâ€Pâ€Vâ€O Catalysts. AICHE Journal, 2013, 59, 2587-2593.	3.6	29
254	Ultrasound assisted interfacial synthesis of gold nanocones. Chemical Communications, 2013, 49, 987-989.	4.1	29
255	Thin Heterojunctions and Spatially Separated Cocatalysts To Simultaneously Reduce Bulk and Surface Recombination in Photocatalysts. Angewandte Chemie, 2016, 128, 13938-13942.	2.0	29
256	Controllable Distribution of Oxygen Vacancies in Grain Boundaries of pâ€Si/TiO ₂ Heterojunction Photocathodes for Solar Water Splitting. Angewandte Chemie - International Edition, 2021, 60, 4034-4037.	13.8	29
257	Role of Fe Species of Ni-Based Catalysts for Efficient Low-Temperature Ethanol Steam Reforming. Jacs Au, 2021, 1, 1459-1470.	7.9	29
258	A comparative study of supported TiO2 catalysts and activity in ester exchange between dimethyl oxalate and phenol. Journal of Molecular Catalysis A, 2004, 222, 183-187.	4.8	28
259	Incorporation of hydrogen in diamond thin films. Diamond and Related Materials, 2009, 18, 1247-1252.	3.9	28
260	The Effect of Adsorbed Water in CO Oxidation on Au/TiO ₂ (110). Journal of Physical Chemistry C, 2011, 115, 2057-2065.	3.1	28
261	Synthesis of Dimethyl Carbonate through Vaporâ€Phase Carbonylation Catalyzed by Pdâ€Doped Zeolites: Interaction of Lewis Acidic Sites and Pd Species. ChemCatChem, 2013, 5, 2174-2177.	3.7	28
262	Influence of CaO precursor on CO2 capture performance and sorption-enhanced steam ethanol reforming. International Journal of Hydrogen Energy, 2019, 44, 20649-20662.	7.1	28
263	Construction of uniform buried pn junctions on pyramid Si photocathodes using a facile and safe spin-on method for photoelectrochemical water splitting. Journal of Materials Chemistry A, 2020, 8, 224-230.	10.3	28
264	Black phosphorus-hosted single-atom catalyst for electrocatalytic nitrogen reduction. Science China Materials, 2021, 64, 1173-1181.	6.3	28
265	Welding of multi-walled carbon nanotubes by ion beam irradiation. Carbon, 2008, 46, 376-378.	10.3	27
266	Adsorption Preference Determines Segregation Direction: A Shortcut to More Realistic Surface Models of Alloy Catalysts. ACS Catalysis, 2019, 9, 5011-5018.	11.2	27
267	Transesterification of dimethyl oxalate with phenol over MoO3/SiO2 catalysts. Journal of Molecular Catalysis A, 2004, 207, 215-220.	4.8	26
268	Coverage Effect on the Activity of the Acetylene Semihydrogenation over Pd–Sn Catalysts: A Density Functional Theory Study. Journal of Physical Chemistry C, 2018, 122, 6005-6013.	3.1	26
269	Transparent Ta2O5 Protective Layer for Stable Silicon Photocathode under Full Solar Spectrum. Industrial & Engineering Chemistry Research, 2019, 58, 5510-5515.	3.7	26
270	Double‧ide Si Photoelectrode Enabled by Chemical Passivation for Photoelectrochemical Hydrogen and Oxygen Evolution Reactions. Advanced Functional Materials, 2021, 31, 2007222.	14.9	26

#	Article	IF	CITATIONS
271	Diamond films with preferred <110> texture by hot filament CVD at low pressure. Diamond and Related Materials, 2008, 17, 2075-2079.	3.9	25
272	Zeolite growth by synergy between solution-mediated and solid-phase transformations. Journal of Materials Chemistry A, 2014, 2, 14360.	10.3	25
273	Effect of bicarbonate on CO2 electroreduction over cathode catalysts. Fundamental Research, 2021, 1, 432-438.	3.3	25
274	Structural change of carbon nanotubes produced by Si ion beam irradiation. Nuclear Instruments & Methods in Physics Research B, 2007, 260, 542-546.	1.4	24
275	Assembly of ordered mesoporous alumina-supported nickel nanoparticles with high temperature stability for CO methanation. Science China Materials, 2015, 58, 9-15.	6.3	24
276	Fast Prediction of CO Binding Energy via the Local Structure Effect on PtCu Alloy Surfaces. Langmuir, 2017, 33, 8700-8706.	3.5	24
277	Theory assisted design of N-doped tin oxides for enhanced electrochemical CO2 activation and reduction. Science China Chemistry, 2019, 62, 1030-1036.	8.2	24
278	Reactivity of Molecularly Chemisorbed Oxygen on a Au/TiO2Model Catalyst. Journal of Physical Chemistry B, 2006, 110, 20337-20343.	2.6	23
279	Hydrogenation of carbon monoxide over cobalt nanoparticles supported on carbon nanotubes. International Journal of Hydrogen Energy, 2011, 36, 8365-8372.	7.1	23
280	Reaction mechanism of dimethyl carbonate synthesis on Cu/\hat{I}^2 zeolites: DFT and AIM investigations. RSC Advances, 2012, 2, 7109.	3.6	23
281	Hollow spherical titanium dioxide nanoparticles for energy and environmental applications. Particuology, 2015, 22, 13-23.	3.6	23
282	Enhanced CO ₂ Electroreduction on Neighboring Zn/Co Monomers by Electronic Effect. Angewandte Chemie, 2020, 132, 12764-12768.	2.0	23
283	Tandem catalysis at nanoscale. Science, 2021, 371, 1203-1204.	12.6	23
284	Sacrificing nothing to reduce CO2. Nature Energy, 2020, 5, 642-643.	39.5	22
285	The Functionality of Surface Hydroxy Groups on the Selectivity and Activity of Carbon Dioxide Reduction over Cuprous Oxide in Aqueous Solutions. Angewandte Chemie, 2018, 130, 7850-7854.	2.0	21
286	Spatial decoupling of light absorption and reaction sites in n-Si photocathodes for solar water splitting. National Science Review, 2021, 8, nwaa293.	9.5	21
287	A comparative study of supported MoO3 catalysts prepared by the new "slurry―impregnation method and by the conventional method: their activity in transesterification of dimethyl oxalate and phenol. Applied Catalysis A: General, 2005, 280, 215-223.	4.3	20
288	Investigations of Catalytic Activity, Deactivation, and Regeneration of Pb(OAc)2for Methoxycarbonylation of 2,4-Toluene Diamine with Dimethyl Carbonate. Industrial & Engineering Chemistry Research, 2007, 46, 6858-6864.	3.7	20

#	Article	IF	CITATIONS
289	Study of inspection on metal sheet with subsurface defects using linear frequency modulated ultrasound excitation thermal-wave imaging (LFM-UTWI). Infrared Physics and Technology, 2014, 62, 136-142.	2.9	20
290	Selective oxidation of methanol to dimethoxymethane over V2O5/TiO2–Al2O3 catalysts. Science Bulletin, 2015, 60, 1009-1018.	9.0	20
291	Role of Sn in Niâ€&n/ <scp>CeO₂</scp> Catalysts for Ethanol Steam Reforming. Chinese Journal of Chemistry, 2017, 35, 651-658.	4.9	20
292	Large-scale fabrication of carbon nanowire networks using kilo-electron-volt ion beam. Diamond and Related Materials, 2008, 17, 365-371.	3.9	19
293	Solar–Wind–Bio Ecosystem for Biomass Cascade Utilization with Multigeneration of Formic Acid, Hydrogen, and Graphene. ACS Sustainable Chemistry and Engineering, 2019, 7, 2558-2568.	6.7	19
294	Chemical looping partial oxidation over FeWO /SiO2 catalysts. Chinese Journal of Catalysis, 2020, 41, 1140-1151.	14.0	19
295	Graphite-to-amorphous structural transformation of multiwalled carbon nanotubes under proton beam irradiation. Materials Letters, 2009, 63, 1505-1507.	2.6	18
296	Annealing Effect on Reactivity of Oxygen-Covered Au(111). Journal of Physical Chemistry C, 2009, 113, 9820-9825.	3.1	18
297	Ethanol steam reforming over Ni/NixMg1â^'xO: Inhibition of surface nickel species diffusion into the bulk. International Journal of Hydrogen Energy, 2011, 36, 326-332.	7.1	18
298	A welding phenomenon of dissimilar nanoparticles in dispersion. Nature Communications, 2019, 10, 219.	12.8	18
299	Origin of Performances of Pt/Cu Single-Atom Alloy Catalysts for Propane Dehydrogenation. Journal of Physical Chemistry C, 2021, 125, 18708-18716.	3.1	18
300	Carbon nanotubes coated by carbon nanoparticles of turbostratic stacked graphenes. Carbon, 2008, 46, 434-439.	10.3	17
301	Enhanced electron field emission of carbon nanotubes by Si ion beam irradiation. Journal Physics D: Applied Physics, 2009, 42, 075408.	2.8	17
302	Mechanistic understanding of hydrogenation of acetaldehyde on Au(111): A DFT investigation. Surface Science, 2012, 606, 1608-1617.	1.9	17
303	Broadband Light Harvesting and Unidirectional Electron Flow for Efficient Electron Accumulation for Hydrogen Generation. Angewandte Chemie, 2019, 131, 10108-10112.	2.0	17
304	Defect-mediated reactivity of Pt/TiO2 catalysts: the different role of titanium and oxygen vacancies. Science China Chemistry, 2020, 63, 1323-1330.	8.2	17
305	Enhanced localized dipole of Pt-Au single-site catalyst for solar water splitting. Proceedings of the National Academy of Sciences of the United States of America, 2022, 119, .	7.1	17
306	Adjusting the Reduction Potential of Electrons by Quantum Confinement for Selective Photoreduction of CO ₂ to Methanol. Angewandte Chemie, 2019, 131, 3844-3848.	2.0	16

#	Article	IF	CITATIONS
307	Activation and Spillover of Hydrogen on Subâ€1â€nm Palladium Nanoclusters Confined within Sodalite Zeolite for the Semiâ€Hydrogenation of Alkynes. Angewandte Chemie, 2019, 131, 7750-7754.	2.0	16
308	Selective Electroreduction of Carbon Dioxide over SnO ₂ â€Nanodot Catalysts. ChemSusChem, 2020, 13, 6353-6359.	6.8	16
309	Anode co-valorization for scalable and sustainable electrolysis. Green Chemistry, 2021, 23, 7917-7936.	9.0	16
310	Moderate Surface Segregation Promotes Selective Ethanol Production in CO ₂ Hydrogenation Reaction over CoCu Catalysts. Angewandte Chemie - International Edition, 2022, 61, .	13.8	16
311	Transesterification of Dimethyl Oxalate with Phenol under SnO2/SiO2Catalysts. Industrial & Engineering Chemistry Research, 2004, 43, 4027-4030.	3.7	15
312	Layer-by-layer films for tunable and rewritable control of contact electrification. Soft Matter, 2013, 9, 10233.	2.7	15
313	Photocatalysis: Selective Deposition of Ag ₃ PO ₄ on Monoclinic BiVO ₄ (040) for Highly Efficient Photocatalysis (Small 23/2013). Small, 2013, 9, 3950-3950.	10.0	15
314	Facile synthesis of Pd@Pt octahedra supported on carbon for electrocatalytic applications. AICHE Journal, 2017, 63, 2528-2534.	3.6	15
315	Modulating the surface defects of titanium oxides and consequent reactivity of Pt catalysts. Chemical Science, 2019, 10, 10531-10536.	7.4	15
316	A bimetallic molybdenum (VI) and stannum (IV) catalyst for the transesterification of dimethyl oxalate with phenol. Catalysis Communications, 2004, 5, 179-184.	3.3	14
317	Large-area and high-density silicon nanocone arrays by Ar+ sputtering at room temperature. Nuclear Instruments & Methods in Physics Research B, 2008, 266, 197-202.	1.4	14
318	Hydroxylâ€Mediated Nonâ€oxidative Propane Dehydrogenation over VO _{<i>x</i>} /γâ€Al ₂ O ₃ Catalysts with Improved Stability. Angewandte Chemie, 2018, 130, 6907-6911.	2.0	14
319	Modulating Photoelectrochemical Water-Splitting Activity by Charge-Storage Capacity of Electrocatalysts. Journal of Physical Chemistry C, 2019, 123, 28753-28762.	3.1	14
320	Synthesis of Interface-Driven Tunable Bandgap Metal Oxides. , 2020, 2, 1211-1217.		14
321	Enabling High Loading in Singleâ€Atom Catalysts on Bare Substrate with Chemical Scissors by Saturating the Anchoring Sites. Small, 2022, 18, e2200073.	10.0	14
322	Tailoring lattice oxygen triggered NiO/Ca9Co12O28 catalysts for sorption-enhanced renewable hydrogen production. Applied Catalysis B: Environmental, 2022, 316, 121642.	20.2	14
323	The effect of specific adsorption of halide ions on electrochemical CO ₂ reduction. Chemical Science, 2022, 13, 8117-8123.	7.4	14
324	Characterization and reactivity of silica-supported bimetallic molybdenum and stannic oxides for the transesterification of dimethyl oxalate with phenol. Journal of Molecular Catalysis A, 2004, 218, 253-259.	4.8	13

#	Article	IF	CITATIONS
325	Characterization and reactivity of stannum modified titanium silicalite TS-1 catalysts for transesterification of dimethyl oxalate with phenol. Journal of Molecular Catalysis A, 2005, 237, 1-8.	4.8	13
326	Synthesis of carbon nanotubes over rare earth zeolites at low temperature. Carbon, 2005, 43, 3015-3017.	10.3	13
327	Investigation on stress distribution of multilayered composite structure (MCS) using infrared thermographic technique. Infrared Physics and Technology, 2013, 61, 134-143.	2.9	13
328	Concentrating and activating carbon dioxide over AuCu aerogel grain boundaries. Journal of Chemical Physics, 2020, 152, 204703.	3.0	13
329	DFT investigations for the reaction mechanism of dimethyl carbonate synthesis on Pd(ii)/β zeolites. Physical Chemistry Chemical Physics, 2013, 15, 13116.	2.8	12
330	Simple Doping, Great Deal: Regulation of Lattice Oxygen for Water Splitting. CheM, 2018, 4, 2739-2741.	11.7	12
331	Reveal the nature of particle size effect for CO2 reduction over Pd and Au. Chinese Journal of Catalysis, 2021, 42, 817-823.	14.0	12
332	Bifunctional Catalyst NiFe–MgAl for Hydrogen Production from Chemical Looping Ethanol Reforming. Energy & Fuels, 2021, 35, 11580-11592.	5.1	12
333	Dataâ€Ðriven Interpretable Descriptors for the Structure–Activity Relationship of Surface Lattice Oxygen on Doped Vanadium Oxides. Angewandte Chemie - International Edition, 2022, 61, .	13.8	12
334	Characterization and activity of stannum modified H^2 catalysts for transesterification of dimethyl oxalate with phenol. Catalysis Today, 2004, 93-95, 377-381.	4.4	11
335	Enhanced Carbonate Formation on Gold. Journal of Physical Chemistry C, 2008, 112, 17631-17634.	3.1	11
336	Study on Lock-in Thermography Defect Detectability for Carbon-Fiber-Reinforced Polymer (CFRP) Sheet with Subsurface Defects. International Journal of Thermophysics, 2015, 36, 1259-1265.	2.1	11
337	Dendritic Hematite Nanoarray Photoanode Modified with a Conformal Titanium Dioxide Interlayer for Effective Charge Collection. Angewandte Chemie, 2017, 129, 13058-13062.	2.0	11
338	Performance comparison among different multifunctional reactors operated under energy self-sufficiency for sustainable hydrogen production from ethanol. International Journal of Hydrogen Energy, 2020, 45, 18309-18320.	7.1	11
339	Arificial Leaves for Solar Fuels. Chinese Journal of Chemistry, 2021, 39, 1450-1458.	4.9	11
340	Transesterification of dimethyl oxalate with phenol over TiO ₂ /SiO ₂ : Catalyst screening and reaction optimization. AICHE Journal, 2008, 54, 3260-3272.	3.6	10
341	CO dissociation induced by adsorbed oxygen and water on Ir(111). Chemical Communications, 2009, , 7300.	4.1	10
342	Exploring the initial oxidation of Pt, Pt3Ni, Pt3Au (111) surfaces: a genetic algorithm based global optimization with density functional theory. Green Chemical Engineering, 2020, 1, 56-62.	6.3	10

#	Article	IF	CITATIONS
343	A study on the SNR performance analysis of laser-generated bidirectional thermal wave radar imaging inspection for hybrid C/GFRP laminate defects. Infrared Physics and Technology, 2020, 111, 103526.	2.9	10
344	Diamond nanorods from nanocrystalline diamond films. Journal of Crystal Growth, 2009, 311, 3332-3336.	1.5	9
345	Effect of non-axisymmetric arc on microstructure, texture and properties of variable polarity plasma arc welded 5A06 Al alloy. Materials Characterization, 2018, 139, 70-80.	4.4	9
346	Golden touch of the nanoparticles. Nature Nanotechnology, 2020, 15, 1-2.	31.5	9
347	Coverageâ€Dependent Behaviors of Vanadium Oxides for Chemical Looping Oxidative Dehydrogenation. Angewandte Chemie, 2020, 132, 22256-22263.	2.0	9
348	Comparative preparation of MoO3/SiO2 catalysts using conventional and slurry impregnation method and activity in transesterification of dimethy oxalate with phenol. Catalysis Letters, 2005, 99, 187-191.	2.6	8
349	Nanosheets: Tungsten Oxide Single Crystal Nanosheets for Enhanced Multichannel Solar Light Harvesting (Adv. Mater. 9/2015). Advanced Materials, 2015, 27, 1579-1579.	21.0	8
350	Determining the Effect of Plasma Preâ€Treatment on Antimony Tin Oxide to Support Pt@Pd and the Oxygen Reduction Reaction Activity. ChemCatChem, 2015, 7, 1543-1546.	3.7	8
351	Effect of Mo content in MoO3/g-Al2O3on the catalytic activity for transesterification of dimethyl oxalate with phenol. Reaction Kinetics and Catalysis Letters, 2004, 83, 113-120.	0.6	7
352	Dispersion and catalytic activity of MoO ₃ on TiO ₂ ‣iO ₂ binary oxide support. AICHE Journal, 2008, 54, 741-749.	3.6	7
353	Photocatalysts: Monoclinic Porous BiVO4Networks Decorated by Discrete g-C3N4Nano-Islands with Tunable Coverage for Highly Efficient Photocatalysis (Small 14/2014). Small, 2014, 10, 2782-2782.	10.0	7
354	Controllable Distribution of Oxygen Vacancies in Grain Boundaries of pâ€ s i/TiO 2 Heterojunction Photocathodes for Solar Water Splitting. Angewandte Chemie, 2021, 133, 4080-4083.	2.0	7
355	Techno-Economic Analysis of a Hybrid Process for Propylene and Ammonia Production. ACS Sustainable Chemistry and Engineering, 2022, 10, 6999-7009.	6.7	7
356	Detection of Fiber Layer-Up Lamination Order of CFRP Composite Using Thermal-Wave Radar Imaging. International Journal of Thermophysics, 2016, 37, 1.	2.1	6
357	Temperature-induced deactivation mechanism of ZnFe ₂ O ₄ for oxidative dehydrogenation of 1-butene. Reaction Chemistry and Engineering, 2017, 2, 215-225.	3.7	6
358	The Evolution of ACS Sustainable Chemistry & Engineering. ACS Sustainable Chemistry and Engineering, 2020, 8, 1-1.	6.7	6
359	Fe2O3/CaO-Al2O3 multifunctional catalyst for hydrogen production by sorption-enhanced chemical looping reforming of ethanol. Biomass Conversion and Biorefinery, 2020, , 1.	4.6	6
360	Reliability Assessment for Time-Slice Enhanced Bidirectional Thermal Wave Radar Thermography of Hybrid C/GFRP Defects. IEEE Transactions on Industrial Informatics, 2021, 17, 6094-6103.	11.3	6

#	Article	IF	CITATIONS
361	A commentary of green hydrogen in MIT Technology Review 2021. Fundamental Research, 2021, 1, 848-850.	3.3	6
362	Artificial photosynthesis of food from CO2. Nature Food, 2022, 3, 409-410.	14.0	6
363	SrO-layer insertion in Ruddlesden–Popper Sn-based perovskite enables efficient CO ₂ electroreduction towards formate. Chemical Science, 2022, 13, 8829-8833.	7.4	6
364	Mechanistic insights into methanolâ€toâ€olefin reaction on an αâ€Mn ₂ O ₃ nanocrystal catalyst. AICHE Journal, 2012, 58, 3474-3481.	3.6	5
365	Reduction of nonspecific binding for cellular imaging using quantum dots conjugated with vitamin E. AICHE Journal, 2014, 60, 1591-1597.	3.6	5
366	Simple Strategies for Fabrication of a Periodic Mesoporous Aluminosilicate with Crystalline Walls. Small, 2014, 10, 4249-4256.	10.0	5
367	Solar Water Splitting: Mechanistic Understanding of the Plasmonic Enhancement for Solar Water Splitting (Adv. Mater. 36/2015). Advanced Materials, 2015, 27, 5444-5444.	21.0	5
368	Overestimated solar water splitting performance on oxide semiconductor anodes. Science China Materials, 2017, 60, 90-92.	6.3	5
369	Why Wasn't My <i>ACS Sustainable Chemistry & Engineering</i> Manuscript Sent Out for Review?. ACS Sustainable Chemistry and Engineering, 2019, 7, 1-2.	6.7	5
370	Catalyst design via descriptors. Nature Nanotechnology, 2022, 17, 563-564.	31.5	5
371	Synthesis of thin diamond films from faceted nanosized crystallites. Current Applied Physics, 2009, 9, 698-702.	2.4	4
372	Interfacial phenomena in (de)hydrogenation reactions. Physical Chemistry Chemical Physics, 2013, 15, 11985.	2.8	4
373	Effective Charge Carrier Utilization in Visible-Light-Driven CO 2 Conversion. Semiconductors and Semimetals, 2017, 97, 429-467.	0.7	4
374	Nanopolyaniline Coupled with an Anticorrosive Graphene as a 3D Film Electrocatalyst for Efficient Oxidation of Toluene Methyl Câ^'H Bonds and Hydrogen Production at Low Voltage. Chemistry - A European Journal, 2019, 25, 6963-6972.	3.3	4
375	Gas–water interface engineered exceptional photoconversion of fatty acids to olefins. Green Chemistry, 2020, 22, 7848-7857.	9.0	4
376	Metal Sputtering Buffer Layer for High Performance Si-Based Water Oxidation Photoanode. ACS Applied Energy Materials, 2020, 3, 8216-8223.	5.1	4
377	Expectations for Papers on Photochemistry, Photoelectrochemistry, and Electrochemistry for Energy Conversion and Storage in <i>ACS Sustainable Chemistry & Engineering</i> . ACS Sustainable Chemistry and Engineering, 2020, 8, 3038-3039.	6.7	4
378	Study of comprehensive compensation system based on fast response magnetically controlled reactor and APF. , 2017, , .		3

#	Article	IF	CITATIONS
379	A new, sustainable process for synthesis of ethylene glycol. Journal of Energy Chemistry, 2018, 27, 949-950.	12.9	3
380	Regioselective metal deposition on polymer-Au nanoparticle hybrid chains. Science China Materials, 2019, 62, 1363-1367.	6.3	3
381	Enhanced C–H bond activation by tuning the local environment of surface lattice oxygen of MoO ₃ . Chemical Science, 2022, 13, 7468-7474.	7.4	3
382	Effect of Mo loading on transesterification activities of MoO <subscript>3</subscript> /g-Al <subscript>2</subscript> O <subscript>3</subscript> catalysts prepared by conventional and slurry impregnation methods. Reaction Kinetics and Catalysis Letters, 2005, 84, 79-86.	0.6	2
383	Effect of Mo loading on transesterification activities of MoO3/γ-Al2O3 catalysts prepared by conventional and slurry impregnation methods. Reaction Kinetics and Catalysis Letters, 2005, 84, 79-86.	0.6	2
384	Intensive irradiation of carbon nanotubes by Si ion beam. Nuclear Science and Techniques/Hewuli, 2007, 18, 137-140.	3.4	2
385	Innentitelbild: Thin Heterojunctions and Spatially Separated Cocatalysts To Simultaneously Reduce Bulk and Surface Recombination in Photocatalysts (Angew. Chem. 44/2016). Angewandte Chemie, 2016, 128, 13818-13818.	2.0	2
386	CO ₂ Electroreduction: Morphological and Compositional Design of Pd–Cu Bimetallic Nanocatalysts with Controllable Product Selectivity toward CO ₂ Electroreduction (Small 7/2018). Small, 2018, 14, 1870031.	10.0	2
387	Expectations for Manuscripts in ACS Sustainable Chemistry & Engineering: Scope Summary and Call for Creativity. ACS Sustainable Chemistry and Engineering, 2020, 8, 16046-16047.	6.7	2
388	Multi-characteristic combination based reliability enhancement of optical bidirectional thermal wave radar imaging for GFRP laminates with subsurface defects. NDT and E International, 2021, 119, 102415.	3.7	2
389	Performance Prediction of Multiple Photoanodes Systems for Unbiased Photoelectrochemical Water Splitting. , 2021, 3, 939-946.		2
390	Enabling High Loading in Singleâ€Atom Catalysts on Bare Substrate with Chemical Scissors by Saturating the Anchoring Sites (Small 19/2022). Small, 2022, 18, .	10.0	2
391	Carbon nanotubes decorated by graphitic shells encapsulated Cu nanoparticles. Applied Physics A: Materials Science and Processing, 2011, 102, 601-604.	2.3	1
392	Frontispiece: Stable Aqueous Photoelectrochemical CO2 Reduction by a Cu2 O Dark Cathode with Improved Selectivity for Carbonaceous Products. Angewandte Chemie - International Edition, 2016, 55, .	13.8	1
393	Uncertainties in Theoretical Description of Well-Defined Heterogeneous Catalysts. Studies in Surface Science and Catalysis, 2017, 177, 541-565.	1.5	1
394	Titelbild: Tuning Cu/Cu ₂ 0 Interfaces for the Reduction of Carbon Dioxide to Methanol in Aqueous Solutions (Angew. Chem. 47/2018). Angewandte Chemie, 2018, 130, 15507-15507.	2.0	1
395	Frontispiece: The Interplay between Structure and Product Selectivity of CO2 Hydrogenation. Angewandte Chemie - International Edition, 2019, 58, .	13.8	1
396	Building Pathways to a Sustainable Planet. ACS Sustainable Chemistry and Engineering, 2022, 10, 1-2.	6.7	1

#	Article	IF	CITATIONS
397	Expectations for Perspectives in ACS Sustainable Chemistry & Engineering. ACS Sustainable Chemistry and Engineering, 2021, 9, 16528-16530.	6.7	1
398	Regulation of Oxygen Activity by Lattice Confinement over Ni Mg1â^'O Catalysts for Renewable Hydrogen Production. Engineering, 2022, , .	6.7	1
399	Nature of the Active Sites of Copper Zinc Catalysts for Carbon Dioxide Electroreduction. Angewandte Chemie, 2022, 134, .	2.0	1
400	Highly (111)-textured diamond film growth with high nucleation density. Nuclear Science and Techniques/Hewuli, 2008, 19, 147-151.	3.4	0
401			